# Rule-Based Landform Classification by Combining Multi-Spectral/Temporal Satellite Data and the SRTM DEM

**Ho, L. T. K..,[1] Yamaguchi, Y.[1] and Umitsu, M.,[2]**
[1]Graduate School of Environmental Studies, Nagoya University, D2-1(510), Furo-cho, Chikusa-ku, Nagoya Japan, 464-8601, E-mail: ho.loan.thi.kim@b.mbox.nagoya-u.ac.jp, yasushi@nagoya-u.jp
[2]Department of Geography, Nara University, 1500 Misasagi-cho, Nara, 631-8502, Japan
E-mail: umitsu.m@gmail.com

**Abstract**
*This study developed a rule-based method for generating a landform classification map of an alluvial plain for further assessment of flood susceptibility. Thresholds of the Modified Normalized Difference Water Index (MNDWI) and land cover characteristics were extracted from Landsat and Advanced Spaceborne Thermal Emission and Reflection Radiometer (ASTER) data. Local relief, average elevation, and channel features were calculated using a Shuttle Radar Topographic Mission Digital Elevation Model (SRTM DEM). Then, relative position indices of polygons were used to classify small-scale landform objects. These inputs were combined based on a rule. The landform classification map by this method was compared to a manual map by visual interpretation. Significant consistence of dominated landform categories between the two maps demonstrates the effectiveness of the rule-base method despite the limitation on spatial resolution of medium-resolution data for detecting some small features. Moreover, the remarkable merits of the rule-based method in comparison with the manual method are its relative time savings, objectivity, and ease of editing.*

## 1. Introduction

A landform classification map plays an important role in the study of the characteristics of many natural phenomena because of the relationship between landforms and these phenomena on a small-scale (micro) landform level, for example, in the case of floods, landslides, and erosion (Speight, 1990). In particular, it is useful for predicting flood-prone areas because the evidence of past flood events is preserved and remains as small-scale landforms (Oya, 2001, Umitsu et al., 2006, Willige, 2007 and Lastra et al., 2008). The "small-scale" term in this study indicates spatial extent (size of the area and landform features) but spatial resolution. In particular, the geomorphological method is effective for developing countries where hydro-meteorological data for generating flood models are usually limited. Ho and Umitsu (2011) developed an integrated method for classifying small-scale landforms in relation to flood inundation by visual interpretation. This manual method used the 90-m-resolution Shuttle Radar Topographic Mission Digital Elevation Model (SRTM DEM) and Landsat Enhanced Thematic Mapper Plus (ETM+) data. Landform units of an alluvial plain were classified by integrating information of elevation and terrain relief derived from the SRTM DEM with spectral characteristics derived from a pair of Landsat images of dry and flood seasons. The results were validated by field investigation, aerial photos, topographic maps, and past-flood images. The results revealed a close relationship between the geomorphological characteristics and flood conditions in this area. Ho and Umitsu (2011) also demonstrated the usefulness of SRTM and Landsat data for geomorphological mapping in locations where topographic and land cover data are insufficient. However, manual landform classification maps generated by visual interpretation rely on human interpretation although they theoretically have more detail and high accuracy. Automatic mapping of landforms using DEMs and satellite images is more time-saving and objective than the manual method (Speight, 1974, 1990 and Van Westen, 1993). Most previous studies of automated landform classification have been conducted on a large scale (e.g., mountains, plateaus, floodplains) or have focused on mountainous or high-elevation areas where topographical

differences are clear and evident (MacMillan et al., 2000, Gallant et al., 2005, Drăgut, and Blaschke, 2006, Iwahashi et al., 2007, Klingseisen, et al., 2008 and Saadat et al., 2008). Studies of automated landform classification maps in alluvial plains are scarcer. The possible reason is the relatively low-relief characteristic of alluvial plains. Thus, it is difficult to extract landforms solely by the use of DEMs. Therefore, it is necessary to combine multi-spectral/temporal data such as Landsat and ASTER data that provide supplemental information about land cover when used in combination with DEMs. For the reasons above, this study makes an effort to address that research challenge by proposing a rule-based method for automatic mapping of small-scale landforms in an alluvial plain using the SRTM DEM with multi-spectral and multi-temporal remotely sensed data.

## 2. Study Areas

The study area is the lower reach of the Vu Gia–Thu Bon river plain in central Vietnam including an alluvial plain formed by fluvial processes in the inland area and a coastal plain formed by aeolian processes in the coastal zone. The two rivers are characterized by a braided and/or anastomosing pattern. In the lowest reach of the plain (the coastal plain), there are sand dunes and bars that align parallel with the coastline (Kubo, 2002). The supply of sandy sediment dominates the river load and governs the flow mechanism of the river as well as its drainage. The central Vietnam receives the highest rainfall in the entire country. The rainy season is from September to December, and the dry season is from January to August. The average annual rainfall in the upland areas of the basin is approximately 3,000 to 4,000 mm, which is much higher than the annual rainfall in the coastal areas (approximately from 1,500 to 2,000 mm) (Quang Nam CFSC, 2009). The elevations of this plain are no greater than 30 m.

## 3. Methodology

### *3.1 Data used and Preprocessing*

The data used are described in Table 1. Only one image in the rainy season (December 21, 2007) was selected. Due to the fact that cloud coverage normally occurs in the rainy season, this rainy-season image showing clear moist surfaces without the cloud coverage is very valuable for classifying landforms in relation to flood inundation in this area. The rest images are in the dry season. The time-series images of the years 1973, 1990, 2001, and 2007 were chosen in comparable periods of time (dry season) to understand dynamic changes in this fluvial system governed by flooding from the past to present. The ASTER image with the higher resolution was used for obtaining land cover characteristics. The SRTM DEM used in this study is WRS (World Reference System) tile, 3 arc-second (90-m) resolution, and filled-finished B set in path/row size (path 124–row 049) with GeoTIFF file format. The SRTM is known as the first ever high-resolution near-global digital elevation data and providing a consistent-quality to give unprecedented opportunities for regional and global applications. SRTM DEMs have proved huge applications on geosciences, especially geomorphology and hydrology (Zandbergen, 2008). Before using SRTM data, pre-processing operations are required. The height overestimation in the SRTM DEM was eliminated over the entire plain by comparing with topographic maps in bare and/or sparse vegetated areas to determine the root mean square error of elevations (Ho and Umitsu, 2011). Then, to remove bias caused by trees and houses from the SRTM elevations after the elimination of height overestimation, the estimated average height of the coverage by trees and houses was subtracted from the elevations within the areas of vegetation and urban; the elevations of the other parts were remained unchanged.

Table 1: Characteristics of the data used

| Data | Date | Resolution (m) | Season |
|---|---|---|---|
| Landsat MSS | June 3, 1973 | 80 | dry |
| TM | August 24, 1990 | 30 | dry |
| ETM+ | March 23, 2001 | 30 | dry |
| ETM+ | March 16, 2007 | 30 | dry |
| ETM+ | December 21, 2007 | 30 | rainy |
| ASTER VNIR | January 31, 2003 | 15 | dry |
| SRTM | February 2000 | 90 | |

The bias by trees and houses was estimated by comparing the SRTM DEM with the 1:25,000 topographic maps of this area via the formula reported by Reuter et al. (2008) as below.

$$\delta_i = z_i^{TOPO} - z_i^{SRTM}$$

Equation 1

*3.2 Specification and Computation of the Inputs*

According to Speight (1974), landforms are determined primarily based on elevation, relief, shape, size, orientation, contextual position, and moisture regimes. Therefore, the following inputs were used in this study:

- Classification of moist conditions by using the Modified Normalized Difference Water Index (MNDWI) and land cover (LC) characteristics derived from Landsat and ASTER data;
- Local relief of object edges (LRoE), average elevation (AVE), and channel features calculated from the SRTM DEM;
- Relative position indices including distances from the centroids of non-water objects to the river, the former river channel, and the dry river bed (DIST) and the ratio of the border of each object with the river, the former river channel, and the dry river bed to the entire border of non-water objects (RBR).

*3.2.1 Classification of moist conditions using the MNDWI*

The MNDWI by Xu (2006) can significantly help to isolate water and moist areas from non-water features and separate water-related areas from urban and sand, which makes the MNDWI better than the original Normalized Difference Water Index (NDWI) by McFeeters (1996).

$$MNDWI = \frac{Green - MIR}{Green + MIR}$$

Equation 2

Ho et al., (2010) demonstrated the effectiveness of the MNDWI for separating moist surface by using thresholds: $-1 \leq MNDWI_{non\text{-}water} < 0 \leq MNDWI_{moist\ soil} < threshold \leq MNDWI_{water} \leq 1$ (Figure 1). This finding suggests an effective method to isolate flooded areas or water-saturated areas with a high potential of being inundated in the rainy season images. In the case of the Landsat images from August 1990, March 2001, and March 2007 (dry season images), the MNDWI thresholds were determined to isolate water from non-water areas for extracting water bodies in each of those years. With the Landsat MSS image of June 1973, the NIR band (band 6) was sliced to determine the threshold to separate river and lake areas in that year. Because the target area is a low-lying alluvial plain, the thresholds of elevation (greater than 30 m), local relief (greater than 30 m), and slope (greater than 10%) (which are the modified definitions of Speight, 1990) were applied to mask the high and upland areas including mountains, hills, plateaus, and upland basins (Figure 1).

*3.2.2 Land cover classification and channel network*

The ISODATA unsupervised classification of the ASTER image was undertaken with 50 clusters. Then, a reclassification process was performed to generate six land cover categories: forest, agricultural land, sandy soil, bare soil, wet land, and urban. Although the more clusters the image is divided into, the better the classified result may be, 50 clusters is appropriate to classify into the six land cover types in this study.

*3.2.3 Extraction of channel features (CFs)*

Channels were also detected using the GRASS GIS function called r.param.scale, which calculates and classifies the terrain features: planar, pit, channel, pass, ridge, and peak (Wood, 1996). The channel extraction performed by this function helped to identify low depressions. These channel features commonly represent channel morphologies such as former river channel, dry river bed, and valley plain areas. In particular, when such low depressions cannot be isolated by the MNDWI classification, land cover classification, or the composite Landsat image, channel features help to separate non-water polygons from areas of extremely low elevation (low depressions) (Figure 2).

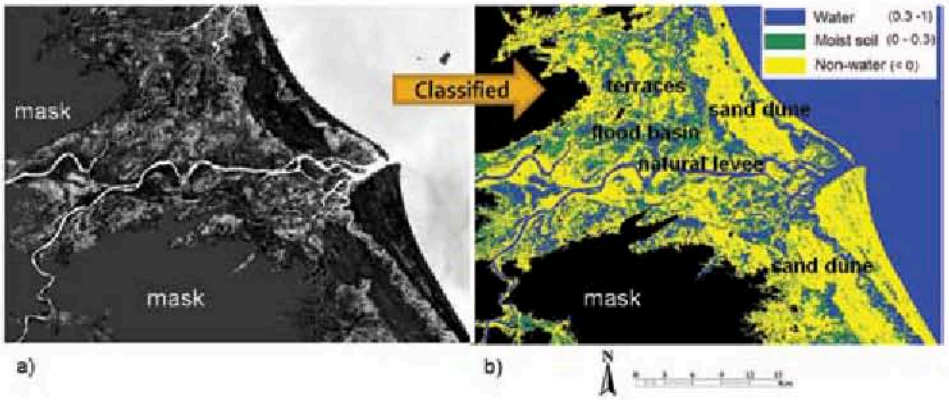


Figure 1: The original MNDWI image of the Landsat ETM+ from December 21, 2007, after the mountains and hills were masked (a). The MNDWI image (b) was categorized into three classes: water (MNDWI 0.3–1), moist soil (MNDWI 0–0.3), and non-water (MNDWI < 0).

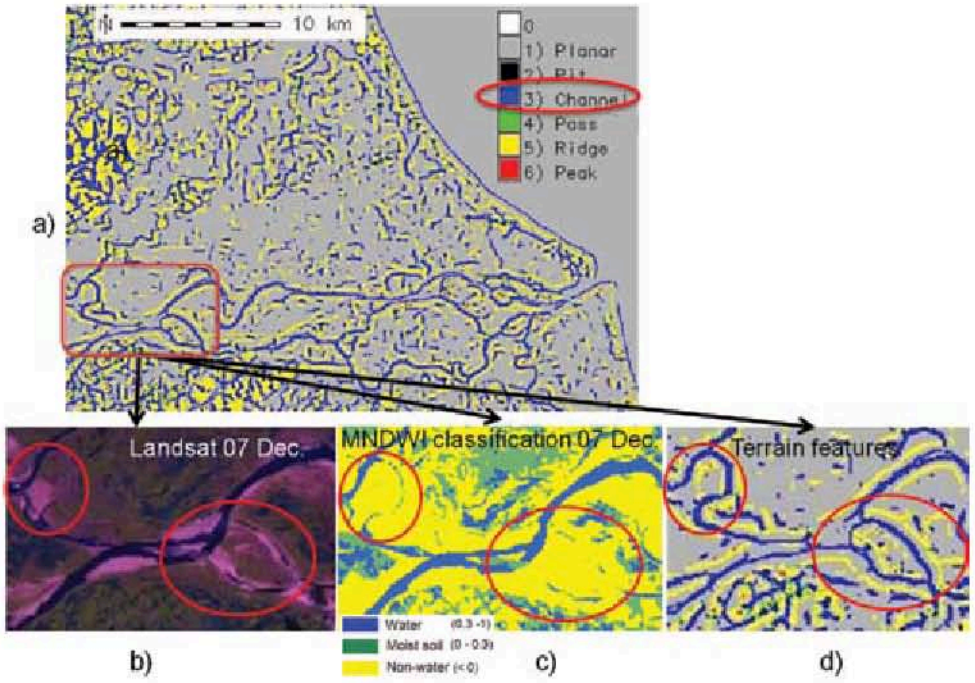


Figure 2: The r.param.scale function can help to extract channel features (low depressions) (a) that are difficult to be detected in the composite Landsat image (b), and they appear as non-water features in the MNDWI classification (c).

*3.2.4 Local relief*

Relief is defined as a difference in elevation between the high and low points of a land surface. Local relief is the relief within a certain area (Coops et al., 1998).

$$localrelief = \max_{i \in C} z_i - \min_{i \in C} z_i \qquad \text{Equation 3}$$

- max $z_i$: the highest elevation value within a moving window C of defined sides (3 x 3, 5 x 5 … size) with a center i,
- min $z_i$: the lowest elevation within this moving window,

The local relief values were calculated by a 3 x 3 square moving window. Local relief is a useful parameter for identifying small-scale landforms because it indicates differences in relative

elevations. Next, average local relief values were calculated within the 120-meter internal buffers of the edges of the non-water polygons.

*3.2.5 Average elevation*

Average elevation is defined as an average value calculated for each target polygon.

$$\overline{z} = \frac{1}{n}(z_1 + z_2 + ... + z_n) = \frac{1}{n}\sum_{i=1}^{n} z_i$$

Equation 4

$\overline{z}$: the average elevation value.
n: the total number of pixels in the target polygon.
$z_1, z_2 \ldots, z_n$: all of the elevation values of the target polygon.

*3.2.6 Relative position indices*

Relative position indices indicate the contextual position of each landform. The relative position relies on the nature of landforms, for example, natural levees are formed along rivers and/or former river channels, whereas sand dunes are situated parallel to the coastline. The relative position indices were used to determine landform objects that have similar characteristics of the above indicators. Relative position indices are represented by the distance to the river, former river channel or dry river bed (DIST) and the ratio of the border of a non-water object with the river to the entire border of that object (RBR) (Figure 3). The RBR indicates how much an object is covered by river, former river channel, and dry river bed areas.

$$RBR = \frac{length\ of\ border\ with\ river}{length\ of\ the\ entire\ border}$$

Equation 5

*3.3 The rule-based landform classification*

The general process of the rule-based landform classification was based on a hierarchical rule by which pixels and objects are separated (Figure 4). The landform categories were classified into three groups: water, moist soil, and non-water areas. The water group consists of permanent water including rivers, lakes, and sea and temporal water stagnating in low areas in the rainy season. The moist soil group consists of low-lying landforms such as flood basins (also back swamp, which is usually used for paddy fields), valley plains, former river channels, dry river beds, and inter-dune marsh. Such low-lying surfaces usually catch overbanking flow, particularly in rainy seasons, thus, these landforms are vulnerable to flooding. In addition, their primary sediment material is clay, which can absorb and maintain water and/or moisture. Therefore, these surfaces commonly appear to be wetter than neighboring higher areas, especially when the paddy fields are not in the growing period and witnessed as bare-moist soil. In contrast, the non-water group comprises high-lying areas with frequently dry conditions consisting of natural levees, terraces, and sand dunes that do not become submerged in flood time. Hence, the non-water landforms are invulnerable to flooding (terraces and sand dunes) or, if they are submerged, are well drained (natural levees). Also, their composition consists of silt and sand as the main sediment materials, which means that they are unlikely to hold water. Such characteristics of these groups are more obvious in the rainy season, when a large amount of rainfall is concentrated on the plain (Ho and Umitsu, 2011). Thus, the wetness of the landform surface is a critical indicator for distinguishing these groups of landforms in an alluvial plain. In short, small-scale landforms (LF) are classified according to the following rules:

- Permanent water (river and lake): if water is indicated in all of the satellite data (MSS 1973 June, TM 1990 August, ETM+ 2001 March, ETM+ 2007 March, and ETM+ 2007 December);
- Flood basin (FB): if (moist soil in MNDWI of ETM+ 2007 December) or (paddy field in the land cover images of ASTER and ETM+ 2007 March);
- Natural levee (NL): if (non-water in MNDWI of ETM+ 2007 December) and (RBR ≥ threshold or DIST ≤ threshold or LRoE ≤ 2 or AVE ≤ 3);
- Former river channel (FRC): if (water in MSS 1973 June or TM 1990 August or ETM+ 2001 March) and (non-water in ETM+ 2007 March or ETM+ 2007 December);
- Dry river bed (DRB): if (LF = channel) and (LC = sand) and (adjacent to river);
- Valley plain (VP): if (LF = channel) and (LF ≠ former river channel and LF ≠ dry river bed);
- Sand dune (SD): if (non-water in ETM+ 2007 December) and (LC dominated by sand) and (2 < LRoE ≤ 3 and DIST > threshold); and
- Terrace (TR): if (non-water in ETM+ 2007 December) and (RBR < threshold and DIST > threshold);
    - else if 3 < LRoE ≤ 4: lower terrace (LTR)
    - else if 4 < LRoE ≤ 5: middle terrace (MTR)
    - else if LRoE > 5: higher terrace (HTR)

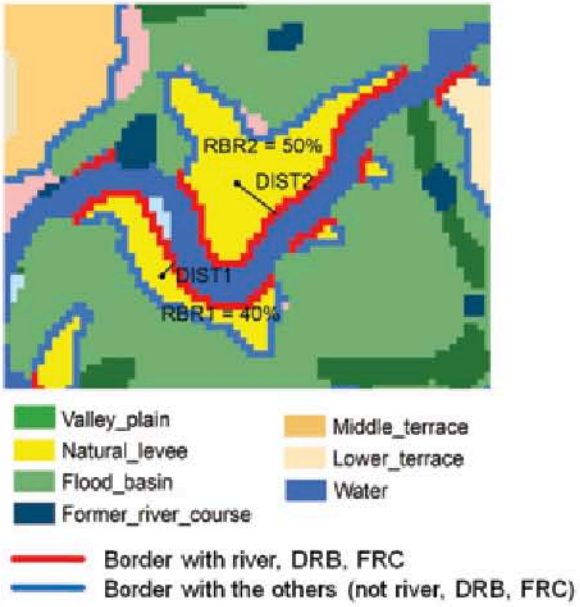


**Figure 3: Distance to river indicates the minimum distance from the centroid of a non-water object to the nearest river, former river channel, or dry river bed objects. The percentage of the total border that borders a river, former river, or dry river (RBR) indicates the water-bordering fraction of a non-water object by dividing the water-bordering length of the border by the entire border length of the object. The DIST and RBR were used to distinguish natural levees from the other non-water features (terraces, sand dunes). See the detailed rules of the classification in the section 3.3.**

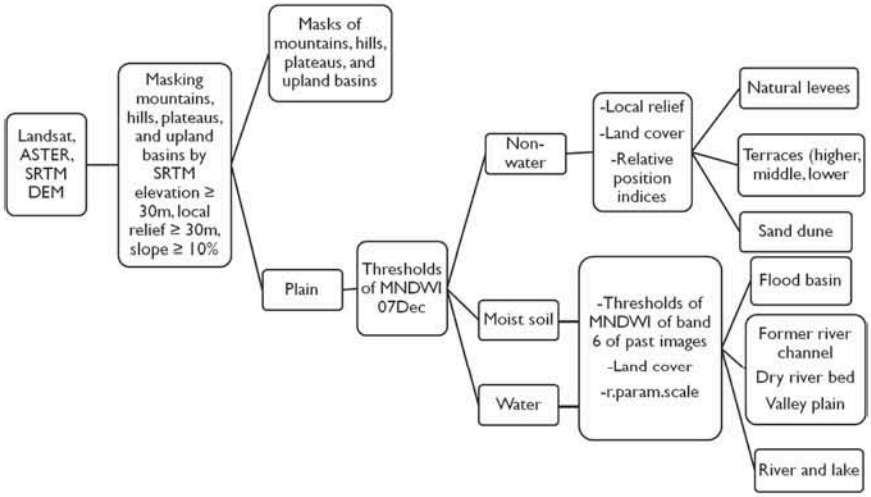


**Figure 4: The flow chart for the rule-based classification of small-scale landforms**

**The thresholds of LRoE, RBR, DIST, and AVE were set based on the characteristics of each landform feature in this area. These indices can be applied for other areas but need to adjust the thresholds depending on the features of landforms in each area.**

**The LRoE threshold was determined depending on the relative height of each terrace type (lower, middle, and higher) that is measured in field and from the topographic map in this study area. The local relief indicates the relative elevation.**

High values of the local relief indicate local scarp of an elevated object whereas its low values indicate the relatively flat surface. Thus, it is used to identify elevation-homogeneous elevated surface such as terraces. The RBR and DIST thresholds were set among non-water and elevated landform features (terraces, sand dunes, and natural levees) after being classified by MNDWI classification and LRoE thresholding. The RBR indicates the coverage degree of a river with a landform object; particularly this index is useful to recognize natural levees. In common, natural levees situate along two sides of a river, as a result empirically about more than two-third portion of their border embedded by a river. Thus, the thresholds of RBR are more than 30%. The DIST index is also useful to identify natural levees that have elongate shape but have uncontinuous borders with a river. Meanwhile the RBR index is more appropriate to distinguish natural levees that have shorter and larger shape and have continuous border with a river. The threshold of DIST is less than approximately 5 pixels equivalent to 150 m with 30 m grid size in this area. The AVE threshold was applied for natural levees situated near deltaic low land near the estuary of the Thu Bon river. Although the rule-based small-scale landform classification in this study is primarily object-based, the salt and pepper effect results from the pixel-based steps of MNDWI classification, river extraction, and land cover classification. Therefore, the rule-based landform classification result was smoothed using the majority method by filtering the most frequently occurring value within the 5 x 5 moving window. Despite the availability of advanced techniques to reduce the "salt and pepper" effect such as Markov Random Field and image segmentation, we did not concentrate on this matter because the main objective of this study is proposing a framework of the rule-based landform classification. Moreover, the majority filter provided acceptable and reasonable accuracy in the previous studies and this study as well.

## 4. Results and Discussion

### *4.1 Evaluation of the Rule-Based Landform Classification Method*

The rule-based landform classification method was evaluated by comparing the statistics of the MNDWI classification with the landform categories of the manual LCM and local relief. The comparisons in Table 2 demonstrate that the MNDWI works well for separating the representative groups and identifying polygon boundaries in the early stages of applying the method because of its good correlation with the manual LCM categories and local relief ranges. First, the non-water, moist soil, and water categories of the MNDWI classification were compared visually with the manual LCM. Figure 5 indicates that the moist soil areas have a high coincidence with the flood basin and valley plain of the manual LCM, which are commonly submerged during times of flooding. For quantitative evaluation, the categories of non-water, moist soil, and water determined by the MNDWI classification in the December 2007 Landsat image were compared with the three landform groups in the manual landform classification map and two ranges of local relief (Table 2). Table 2 reveals good agreement between the MNDWI classification results and the landform groups on the manual landform classification map. The percentage of agreement between the moist soil class and the landform groups of FB, VL, FRC, and DRB on the manual map is 79.74%, whereas the agreement between the non-water class and the landform groups of NL, TR, and SD on the manual map is 68.49%. The former group is located at low elevations and has a high inundation potential, whereas the latter group is at high elevations and has a low inundation potential in the rainy season. On the one hand, a comparison of moist soil and non-water areas and local relief shows that the moist soil class covers only 19.62% of local relief values 2 > m, whereas moist soil covers 80.38% of local relief values $\leq$ 2 m. The non-water class covers 34.62% of local relief values > 2 m and 65.38% of local relief values $\leq$ 2 m. From these numbers, it can be inferred that most of the high local relief values are distributed within the non-water class and that such high local relief values exist at the boundaries of polygons. On the other hand, a large amount of local relief values $\leq$ 2 m belongs to the non-water class because the inner areas of the non-water features (terraces, natural levees, and sand dunes), with the exception of the boundaries of the polygons, are commonly flat, and hence the local relief of such inner areas is usually low. In general, although the low local relief values ($\leq$ 2 m) dominate in either the non-water or the moist soil class because of the flatness and low relief of most of the landform surfaces in the alluvial plain, high local relief values (> 2 m) are more dominant in the non-water class (distributing at the edges of the non-water features) than in the moist soil class.

Table 2: Statistics of the non-water, moist soil, and water classes of MNDWI classification compared with landform categories and local relief

| | | MNDWI classification | | |
|---|---|---|---|---|
| | | Non-water (%) | Moist soil (%) | Water (%) |
| Manual LCM | Flood basin, valley plain, former river channel and dry riverbed | 29.89 | 79.74 | 19.55 |
| | Natural levee, terrace and sand dune | 68.49 | 17.03 | 8.34 |
| | River and lake | 1.62 | 3.23 | 72.11 |
| Local relief | ≤ 2 m | 65.38 | 80.38 | |
| | > 2 m | 34.62 | 19.62 | |

*4.2 The Rule-Based Landform Classification Map*

The scale of the rule-based landform classification map is designated based on the pixel size of Landsat TM/ETM+ (30 m). According to Hengl (2006), the cell size is equal to 0.5 mm on a paper map. In other words, the 30-m resolution of the grid of the rule-based map corresponds to a 1:60,000-scale map. The "mountain and hill" category did not exist in the rule-based landform classification map because it was masked, as described previously. The same mask was applied to the manual map to make it consistent with the rule-based map. However, several areas of mountain and hill remained on the manual map.

*4.3 Comparing the Rule-Based Landform Classification Maps with the Manual One*

Small-scale landform features of the rule-based LCM were compared with those of the manual LCM that was validated by Ho and Umitsu (2011). These two maps were compared by considering only the landform categories existing on both maps. The rule-based LCM shows a high correlation with the manual LCM by visual comparison (Figure 6). The overall similarity of the rule-based map compared to the manual one is 58.1% done by the overlay statistical method. This modest accuracy is resulted from 1) the subjectivity existing in the manual map that is overcome by the rule-based method and 2) the limitations and difficulties of the rule-based mapping method for identifying small objects. The discussion focuses on the main landform categories that dominate this alluvial plain and contribute to explain the flood inundation conditions such as terraces, flood basin, natural levees, sand dunes (high accuracy), former river channel, dry river bed, and valley plain (lower accuracy). The high-accuracy group has significant similarities, which demonstrates the efficiency of the rule-based method for the landform classification. The lower-accuracy group accounts for the modesty of the overall similarity. In other words, it indicates the limitation and difficulties of the rule-based mapping method using medium resolution data. In addition, the lower-accuracy group also reveals the subjectivity of landform classification by the manual method. Although the manual landform classification map was validated with 90% accuracy by the field investigation combined with aerial photos and topographic maps (Ho and Umitsu, 2011), there are some features and/or objects that make confusing. Those can be identified evidently by the rule-based process. Because Ho and Umitsu (2011) investigated and verified randomly around the study area where the authors could access, and allocated most of the categories of the landform but did not cover all of objects. Therefore, for instance, the large areas of each level of terraces were investigated, but the other small parts of terraces were paid less attention. In other studies (Speight, 1974, 1990 and Van Westen, 1993) and our opinion, the field investigation, interpretation of aerial photos, and topographic maps are the key processes of the manual method, but at the same time, are affected by human subjectivity. Furthermore, the boundary delineation of the landform objects by the manual method normally relies on the interpretation and experiences of the person creating the map (Klingseisen et al., 2008). Therefore, even the manual map was validated, its boundary delineation has a certain degree of subjectivity. These shortcomings can be overcome by the rule-based method.

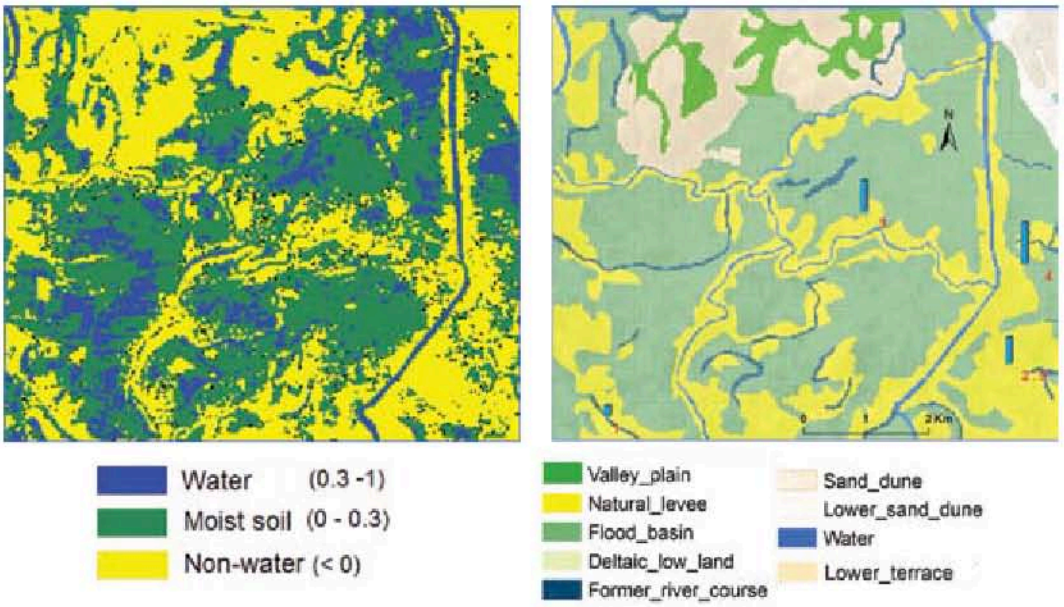


**Figure 5: The left-hand side shows the MNDWI after categorization into three classes, and the right-hand side shows the manual landform classification map. With the exception of permanent water such as rivers and channels, we can see only temporal water in the moist soil areas. The blue (temporal water) and green parts (moist soil) of the MNDWI image coincide well with the flood basin in the manual landform classification map. The yellow areas (non-water) in the left-hand image have patterns similar to those indicating the natural levees and terraces in the right-hand map**

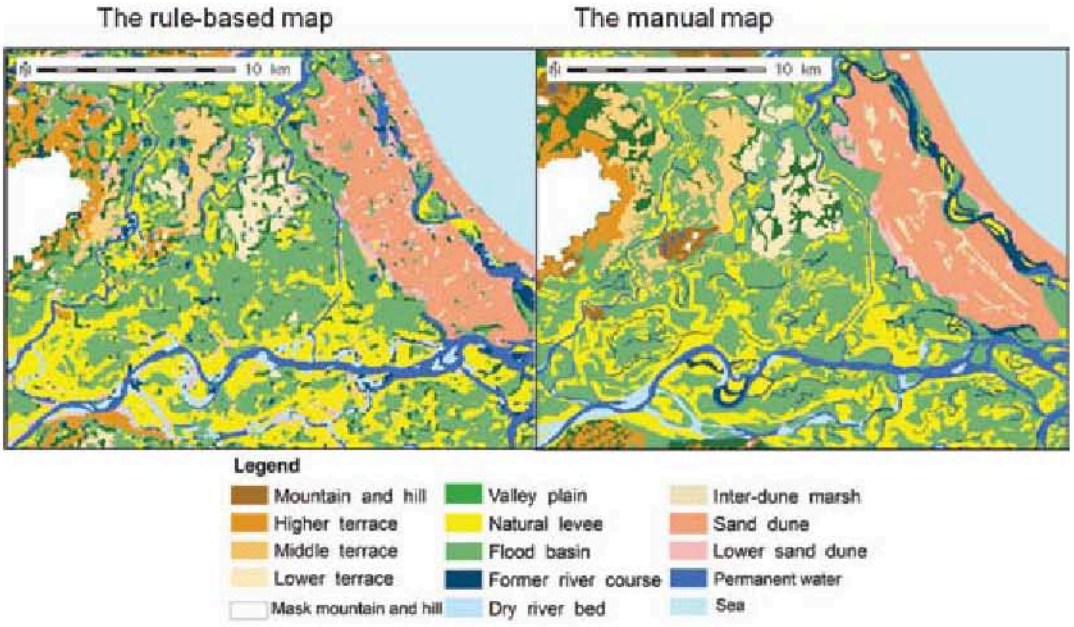


**Figure 6: The rule-based small-scale landform classification map (left) compared to the manual map (right).**

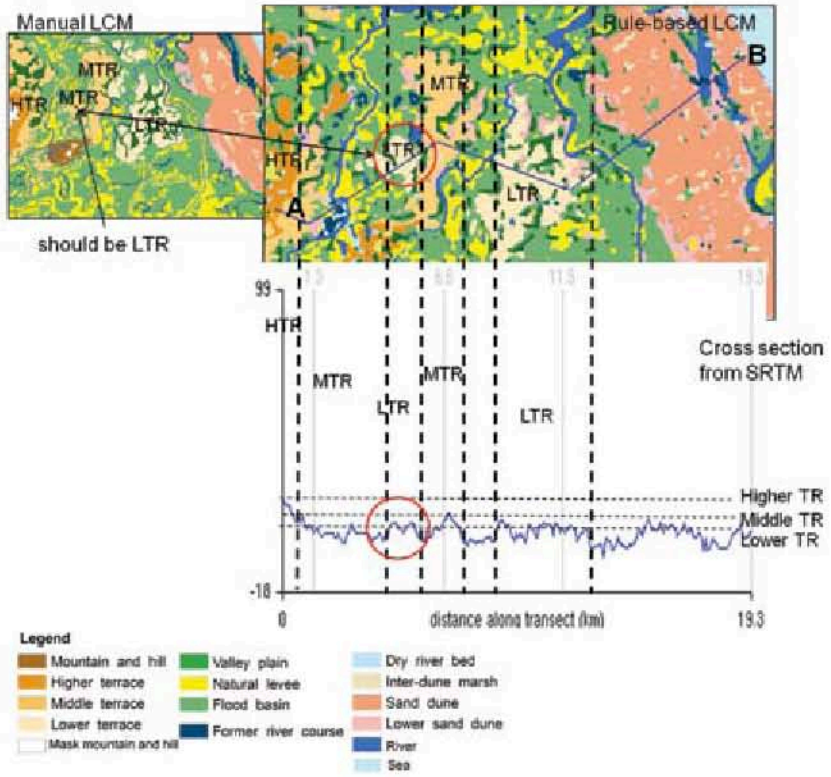


Figure 7: The lower terrace (the upper red circle) was classified on the rule-based LCM (right), but it appears as a middle terrace on the manual LCM (left). The cross section derived from the SRTM DEM affirms that the average level of this lower terrace (the lower red circle) is lower than that of the middle and higher terraces.

*4.3.1 Extraction of Terraces*

The similarity of terraces between the rule-based and manual LCMs is 37.9% for the higher terrace, 66.7% for the middle terrace, and 57.5% for the lower terraces. Misclassification may occur among higher, middle, and lower terraces of the manual LCM, which can cause low accuracy for each terrace classification of the rule-based LCM. However, these misclassifications are likely caused by the subjective interpretation of various levels of terraces when creating the manual map. Figure 7 presents an example of the misclassification of a lower terrace. Another statistic by comparing the total area of the terraces of the rule-based LCM with that of the manual LCM reveals that the total similarity of the terraces is higher than 80%. The classification of terrace levels is a challenge. In common, most of the landform categories are rather evident to distinguish because their characteristics are clear. Nevertheless, the cases between lower and middle terraces and between lower terraces and natural levees are special and more difficult to classify even by using aerial photo stereo-scoping although their separation is crucial for understanding flood conditions of a floodplain.

*4.3.2 Extraction of Flood Basins and Natural Levees*

The accuracy of the flood basin classification of the rule-based LCM is 67.4%, and the misclassification of the flood basin as the valley plain and the former river channel is 5.1% and 4.7%, respectively, on the manual LCM. However, the flood-affected degree of the valley plain and the former river channel is similar the flood basin. Therefore, this misclassification causes inconsiderable problems in the prediction of flood susceptibility. The rate of misclassification of the flood basin as the natural levee is 17.2%. Such natural levees are small and narrow. They appear as moist soil in the MNDWI classification, are usually submerged in times of flooding, and are not useful for human settlement. Thus, this misclassification is also unremarkable for the goal of flood assessment.

*4.3.3 Extraction of sand dunes*

The comparison demonstrated that sand dunes on the rule-based map have 87.5% coincidence with those on the manual map. This high agreement is a result of the stability, large size, and clear boundaries of the sand dunes.

*4.3.4 Extraction of River Networks, Former River Channels, Dry River beds and Valley Plains*

The river network determined by multi-temporal images was classified more precisely than those on the manual map based on a single-year image. The recent river network can be extracted from the present images or the newest image of a dataset. Dry river beds and former river channels have modest accuracies due to the limitation on the data used resolution. Those two landform categories commonly comprises small objects that are difficult to be extracted based on the SRTM DEM and Landsat data, but can be identified by visual interpretation. However, the larger objects of dry river beds and former river channels can be identified advantageously and subjectively by the past river network, which can be derived from the past images. Valley plains on the two maps were visually compared and showed good coincidence with the channel feature by the function r.param.scale in spite of less similarity with that of the manual map.

## 5. Conclusions

The rule-based landform classification method achieved by combining the SRTM DEM and multi-temporal satellite images is effective and promising for classifying small-scale landforms in alluvial plains. Furthermore, this rule-based method is objective, simple to edit, and saves much more time than the manual method. The remarkable advantage of this method is that it produces more objective classifications than a manual method because it quantifies the characteristics derived from satellite images and the SRTM DEM. Mountains and hills are defined (masked) by thresholds of elevation, local relief, and slope, and thus more reliable. Sand dunes are identified with high accuracy. Terraces are separated objectively by local relief and average elevation. Flood basins are classified in close relationship to the moist condition, which makes the data convenient for predicting areas that might be affected by flooding. The use of multi-temporal satellite images helps to classify river network more precisely and to identify dry river beds and former river channel areas effectively. However, limitations on the spatial resolution of satellite data and the SRTM DEM create difficulty in identifying small-size landforms such as narrow rivers, former river channels, dry river beds, and narrow natural levees that can be identified well by visual interpretation. These limitations have only insignificant effects on the prediction of areas that are susceptible to flooding. Thus, this method is effective and suitable for flood hazard assessment. In particular, this method would be useful in developing countries because it enables the creation of landform classification maps that are consistent with manual LCMs by visual interpretation.

**Acknowledgments**

We sincerely thank the Global Earth Observation Grid (GEO Grid) of the National Institute of Advanced Industrial Science and Technology (AIST) for providing the ASTER data for our research. We are also grateful to the Global Land Cover Facility (GLCF) of NASA for providing the SRTM DEM and the U.S. Geological Survey (USGS) for providing Landsat data. We greatly thank the developers of the open source GRASS GIS which is really useful for processing the data in our study.

## References

Coops, N. C., Gallant, J. C., Loughhead, A. N., MacKey, B. J., Ryan, P. J., Mullen, I. C. and Austin, M. P., 1998, Developing and Testing Procedures to Predict Topographic Position from Digital Elevation Models (DEMs) for Species Mapping (Phase 1). *Environment Australia, CSIRO Forestry and Forest Products*, Client Report, 271, 56.

Drăgut, L. and Blaschke, T., 2006, Automated Classification of Landform Elements using Object-Based Image Analysis. *Geomorphology*, 81, 330-344.

Gallant, A. L., Brown, D. D. and Hoffer, R. M., 2005, Automated Mapping of Hammond's Landforms. *IEEE Geoscience and Remote sensing Letters*, 2 (4), 384-388.

Hengl, T., 2006, Finding the Right Pixel Size. *Computers & Geosciences*, 32 (9), 1283–1298.

Ho, T. K. L ., Umitsu, M. and Yamaguchi, Y., 2010, Flood Hazard Mapping by Satellite Images and SRTM DEM in the Vu Gia – Thu Bon Alluvial Plain, Central Vietnam. *International Archives of the Photogrammetry, Remote Sensing and Spatial Information Science*, 38 (Part 8), 275-280.

Ho, T. K. L. and Umitsu, M., 2011, Micro-Landform Classification and Flood Hazard Assessment of the Thu Bon Alluvial Plain, Central Vietnam via an Integrated Method Utilizing Remotely Sensed Data. *Applied Geography*, 31, 1082-1093.

Iwahashi, J. and Pike, R. J., 2007, Automated Classifications of Topography from DEMs by an Unsupervised Nested-Means Algorithm and a Three-Part Geometric Signature. *Geomorphology*, 86, 409 – 440.

Klingseisen, B., Metternichtc, G. and Paulus, G., 2008, Geomorphometric Landscape Analysis using a Rule-Based GIS-Approach. *Environmental Modelling & Software*, 23 (1), January 2008, 109-121.

Kubo, S., 2002, Geomorphological features of the Thu Bon River Plain, Central Vietnam, and their Relations on Flood Hazards in 1999. A*cademic research, School of Education, Waseda University*, 50, 1-12.

Lastra, J., Fernández, E., Díez-Herrero, A. and Marquínez, J., 2008, Flood Hazard Delineation Combining Geomorphological and Hydrological Methods: an Example in the Northern Iberian Peninsula. *Natural Hazards*, 45 (2), 277–293.

MacMillan, R. A., Pettapiece, W. W., Nolan, S. C. and Goddard, T. W., 2000, A Generic Procedure for Automatically Segmenting Landforms into Landform Elements using DEMs, Heuristic Rules and Fuzzy Logic. *Fuzzy Sets and Systems*, 113, 81-109.

McFeeters, S. K., 1996, The use of the Normalized Difference Water Index (NDWI) in the Delineation of Open Water Features. *International Journal of Remote Sensing*, 17 (7), 1425-1432.

Oya, M., 2001, *Applied Geomorphology for Mitigation of Natural Hazards* (Kluwer Academic Publishers in Dordrecht., Boston), 167.

Quang Nam Committee for Flood and Storm Control (CFSC), 2009, The Strategies for Integrated Natural Disaster Management in Quang Nam Province until 2020. (In Vietnamese), *Tam Ky City*, May 2009.

Reuter, H. I., Hengl, T., Gessler, P. and Soille, P., 2008, Preparation of DEMs for Geomorphometric Analysis. In *Geomorphometry: Geomorphometry: Concepts, Software, Applications,* edited by Hengl, T. and Reuter, H.I . (Developments in Soil Science, 33, Elsevier), 87 – 120.

Saadat, H., Bonnell, R., Sharifi, F., Mehuys, G., Namdar, M. and Ale-Ebrahim, S., 2008, Landform Classification from a Digital Elevation Model and Satellite Imagery. *Geomorphology*, 100, 453 – 464.

Speight, J. G., 1974, A Parametric Approach to Landform Regions. *Progress in Geomorphology*, Special Publication, Institute of British Geographers, Alden and Mowbray Ltd at the Alden Press, Oxford, 7, 213–230.

Speight, J. G., 1990, Landform. In *Australian Soil and Land Survey Field Handbook*, 3rd edition, edited by McDonald, R.C., Isbell, R.F., Speight, J.G., Walker, J., & Hop, M.S., (CSIRO Publishing), 9–57.

Umitsu, M., Hiramatsu, T. and Tanavud, C., 2006, Research on the Flood and Micro Landforms of the Hat Yai Plain, Southern Thailand with SRTM Data and GIS. *Geomorphological Union*, 27(2), 205-219.

Van Westen, C., 1993, *GISSIZ: Training package for Geographic Information Systems in Slope Instability Zonation*, (Enschede, The Netherlands ITC Publication), 15, 245.

Willige, B. T., 2007, Flooding Risk of Java, Indonesia. *Proceedings of forum DKKV/CEDIM: Disaster reduction in climate change*, October 15 – 16, 2007.

Wood, J., 1996, *The Geomorphological Characterisation of Digital Elevation Models. PhD*. Thesis. (Leicester, UK: Department of Geography, University of Leicester), 185.

Xu, H., 2006, Modification of Normalised Difference Water Index (NDWI) to Enhance Open Water Features in Remotely Sensed Imagery. *International Journal of Remote sensing*, 27 (14), 3025-3033.

Zandbergen, P., 2008, Applications of Shuttle Radar Topography Mission Elevation Data. *Geography Compass*, 2/5 (2008), 1404–1431.

**Websites**

GEOGrid - ASTER source, https://big.geogrid.org/ (Assessed April, 2010)

LANDSAT sources, http://glovis.usgs.gov/ (Accessed April 2010)

SRTM source, http://ftp.glcf.umd.edu/data/srtm/ (Accessed 10 September 2008)